Temperature Dependence and Thermodynamic Properties of Ca^{2+} Sparks in Rat Cardiomyocytes

Yu Fu, Guang-Qin Zhang, Xue-Mei Hao, Cai-Hong Wu, Zhen Chai, and Shi-Qiang Wang
National Key Laboratory of Biomembrane and Membrane Biotechnology, College of Life Sciences, Peking University, Beijing 100871, China

ABSTRACT To elucidate the temperature dependence and underlying thermodynamic determinants of the elementary Ca^{2+} release from the sarcoplasmic reticulum, we characterized Ca^{2+} sparks originating from ryanodine receptors (RyRs) in rat cardiomyocytes over a wide range of temperature. From 35°C to 10°C, the normalized fluo-3 fluorescence of Ca^{2+} sparks decreased monotonically, but the $\Delta[Ca^{2+}]_i$ were relatively unchanged due to increased resting $[Ca^{2+}]_i$. The time-to-peak of Ca^{2+} sparks, which represents the RyR Ca^{2+} release duration, was prolonged by 37% from 35°C to 10°C. An Arrhenius plot of the data identified a jump of apparent activation energy from 5.2 to 14.6 kJ/mol at 24.8°C, which presumably reflects a transition of sarcoplasmic reticulum lipids. Thermodynamic analysis of the decay kinetics showed that active transport plays little role in early recovery but a significant role in late recovery of local Ca^{2+} concentration. These results provided a basis for quantitative interpretation of intracellular Ca^{2+} signaling under various thermal conditions. The relative temperature insensitivity above the transitional 25°C led to the notion that Ca^{2+} sparks measured at a "warm room" temperature are basically acceptable in elucidating mammalian heart function.

INTRODUCTION

Intracellular Ca^{2+} transients that control muscle contractions and other cell activities are composed of the elementary Ca^{2+} events, Ca^{2+} sparks, originated from ryanodine receptor (RyR) Ca^{2+} release channels in the sarcoplasmic reticulum (SR) (for review, see Bers (1) and Berridge et al. (2)). Since their discovery (3), Ca^{2+} sparks have been found in cardiac, skeletal, and smooth muscle cells, glias, and neurons (4–8) and provide molecular interpretations for intracellular Ca^{2+} signal transduction. However, despite extensive studies of Ca^{2+} sparks during the past decade, most measurements of Ca^{2+} sparks were performed under room temperature (22 ~ 25°C). One of a few studies that measured Ca^{2+} sparks with temperature control, to our knowledge, was reported by Wier et al. (9), who demonstrated Ca^{2+} sparks in quiescent rat trabeculae at 33°C and suggested that Ca^{2+} sparks can occur above room temperature and are not restricted to dissociated myocytes. A comparison of Ca^{2+} sparks at different temperatures was not seen until the recent work by Ferrier et al. (10), who showed that a temperature increase from 22°C to 37°C significantly reduces the normalized fluo-3 fluorescence ($\Delta F/F_0$), time-to-peak, and frequency of Ca^{2+} sparks in mouse cardiomyocytes. Their data provide valuable information for Ca^{2+} sparks at mammalian body temperature (although we have different results in this study), yet the full picture of temperature dependence of Ca^{2+} sparks is not known.

Temperature has comprehensive influence on most (if not all) biochemical processes, including intracellular Ca^{2+} signaling. In mammals, neural transmission, muscle contraction, and heart beating, which depend heavily on intracellular Ca^{2+} dynamics, are most vigorous at their normal body temperature. Lowering temperature not only slows down the kinetics of neuromuscular activities but also causes metabolic and functional problems. In humans and dogs, for example, a hypothermia lower than 25 ~ 28°C usually results in severe ventricular fibrillation and cardiac arrest (11), a problem that has restricted the clinical application of cryo-anesthesia. When isolated and bathed in an artificial environment, cardiac myocytes from rats and rabbits exhibit slower contractions at lower temperatures and gradually lose contractility when the temperature is below ~20°C (12,13). Measurement of intracellular free Ca^{2+} concentration ($[Ca^{2+}]_i$) showed that the amplitude of Ca^{2+} transient decreases dramatically at low temperatures, implying a dysfunction of the excitation-contraction coupling apparatus (14). Because Ca^{2+} sparks represent the elementary Ca^{2+} release events, understanding the temperature dependence of Ca^{2+} sparks is fundamental for elucidating the cardiac function under various physiological conditions, including euthermia and hypothermia.

In this study, we measured Ca^{2+} sparks in rat ventricular myocytes over a wide temperature range from 35°C to 10°C. We quantified the temperature sensitivity of Ca^{2+} spark morphology and kinetics and analyzed the underlying determinants from the thermodynamic point of view.

METHODS

Cell preparation

Ventricular cardiac myocytes from adult Sprague-Dawley rats (age, 2–3 months; weight, 225–300 g) were prepared as previously reported (15,16). Briefly, the hearts were rapidly excised from the animals under ether

Submitted May 20, 2005, and accepted for publication July 21, 2005.

Address reprint requests to Shi-Qiang Wang, E-mail: wsq@pku.edu.cn; or Xue-Mei Hao, E-mail: haoxm@pku.edu.cn.

0006-3495/05/10/2533/09 $2.00

doi: 10.1529/biophysj.105.067074

anesthesia and perfused for 5 min at 37°C with a calcium-free buffer containing (in mM): 110 NaCl, 4 KCl, 1.2 $MgCl_2$, 1.2 NaH_2PO_4, 20 $NaHCO_3$, 30 taurine, 10 glucose, aerated with 95% O_2 + 5% CO_2, pH 7.35. The tissue was then digested in a buffer containing 0.5 mg/ml collagenase (Sigma (St. Louis, MO), Type 1A), 1% bovine serum albumin (Sigma, fraction V), and 75 μM Ca^{2+} for 15 min. The ventricle was then cut into small pieces and incubated in digesting solution. Finally the myocytes were harvested and stored in Tyrode's solution which contained (in mM): 135 NaCl, 4 KCl, 1.0 $CaCl_2$, 1.2 $MgCl_2$, 1.2 NaH_2PO_4, 10 glucose, 5 HEPES, pH 7.35 adjusted by NaOH. Ca^{2+} indicators were loaded into cells before experiments by exposing the cells to 2.5 μM fluo-3 acetoxymethyl ester or indo-1 acetoxymethyl ester (Molecular Probes, Eugene, OR) in Tyrode's solution for ~5 min or 20 min, respectively, in the dark at 37°C.

Recording and analysis of Ca^{2+} sparks

In Ca^{2+} spark recording, the fluorescence of fluo-3-loaded cells was measured with a Zeiss LSM510 confocal microscope equipped with an argon laser and a 40×, 1.3 numerical aperture oil immersion objective and adjusted to axial and radial resolutions of 1.5 and 0.5 μm, respectively. The cells were scanned with a 488 nm laser, and the fluorescence was separated by a 495-nm dichroic mirror in combination with a 500-nm long-pass filter. Line-scan (*x-t*) imaging was performed with a sampling rate of 0.78 ms per scan line.

Ca^{2+} spark analysis was performed using an IDL routine as reported previously (17,18). In brief, after a minimal (3 × 3) smooth, the original fluorescent data (F) were normalized by resting fluorescence (F_0). The threshold for the program to pick up events was set at 1.25 F/F_0. The amplitude, full width at half-maximum (FWHM), full duration at half-maximum (FDHM), time-to-peak, rate-of-rise, and half-decay time of Ca^{2+} sparks were determined automatically with the routine. When necessary, the $\Delta[Ca^{2+}]_i$ of Ca^{2+} sparks were calculated using the formula

$$\Delta[Ca^{2+}]_i = \frac{K_d R C_0}{K_d - R C_0 + C_0} - C_0, \quad (1)$$

in which $R = F/F_0$, C_0 is the resting $[Ca^{2+}]_i$ measured as described below, and K_d is the dissociation constant of fluo-3 (3). As the K_d of fluo-3 is almost temperature independent at physiological pH (19), taking into account the influence of intracellular environment on K_d of fluo-3 (20), an approximate value of 1 μM was used to calculate the $\Delta[Ca^{2+}]_i$.

Measurement of resting Ca^{2+} concentration

Most previous calculations of the intracellular free Ca^{2+} concentration ($[Ca^{2+}]_i$) corresponding to Ca^{2+} sparks were based on an assumed value of resting $[Ca^{2+}]_i$ (usually set at 100 nM). However, the resting $[Ca^{2+}]_i$ itself changes significantly with temperature (14,21). To access the $[Ca^{2+}]_i$ profile of Ca^{2+} sparks at different temperatures, we used the ratiometric Ca^{2+} indicator, indo-1, to determine the resting $[Ca^{2+}]_i$ in ventricular myocytes under otherwise the same experimental settings as in spark measurement. Cells were loaded with indo-1 by exposure to 2.5 μM indo-1/AM in Tyrode's solution for ~15 min in the dark at 37°C. The indo-1 fluorescence was visualized and measured by an ASCS Meridian 575 UV confocal microscope equipped with a UV laser. The fluorescence was separated by a 450-nm dichroic mirror into two channels with 485/45 nm and 405/45 nm bandpass filters, respectively. The intracellular Ca^{2+} concentration was calculated by the formula

$$[Ca^{2+}] = K_d \beta \frac{R - R_{min}}{R_{max} - R}, \quad (2)$$

in which R is the ratio of fluorescence detected at 405 nm versus that detected at 480 nm, R_{max} and R_{min} were the R in Ca^{2+}-free and Ca^{2+}-saturated buffers, respectively, and β is the ratio of 480 nm fluorescence in Ca^{2+}-free versus in Ca^{2+}-saturated buffers. The dissociation constant, K_d, of indo-1 at different temperatures was determined as previously reported (15).

Temperature control

To control the bathing temperature while using an inverted confocal microscope, we designed a temperature-control chamber in which a circular glass cannula was fixed on the center of a coverslip-bottomed petri culture dish. The glass cannula formed a 0.5 ml reservoir for bathing the cells. Temperature was controlled by perfusing the circular glass cannula with a Cole-Parmer refrigerated circulator. A tiny bithermal thermistor probe was attached on the glass bottom of the dish to monitor the temperature. When there was 0.3 ml solution in the chamber, the temperature difference between the center and the periphery of the useful area of the coverslip was <0.5°C. In the experiments, temperature was altered alternately from 35°C to 10°C and from 10°C to 35°C to avoid time-dependent effects. At each temperature, cells were allowed at least 5 min for equilibrium.

Statistics

The data are presented as mean ± SE. One-way analysis of variation with repeated measures was used to analyze the significance of the effects of temperature and other factors. $p < 0.05$ was considered significant.

RESULTS

Using confocal microscopy in line-scan mode, spontaneous Ca^{2+} sparks were recorded at every 5°C from 35°C to 10°C. Fig. 1 *A* shows typical line-scan images recorded at 35°C, 25°C, and 15°C, respectively. With the decrease in temperature from 35°C, the frequency of Ca^{2+} sparks increased progressively until reaching a maximum at 15°C (Fig. 1 *B*). For a clear demonstration of the temperature-dependent change of Ca^{2+} spark morphology, we averaged 64 Ca^{2+} sparks randomly sampled at 35°C, 25°C, and 15°C, respectively,

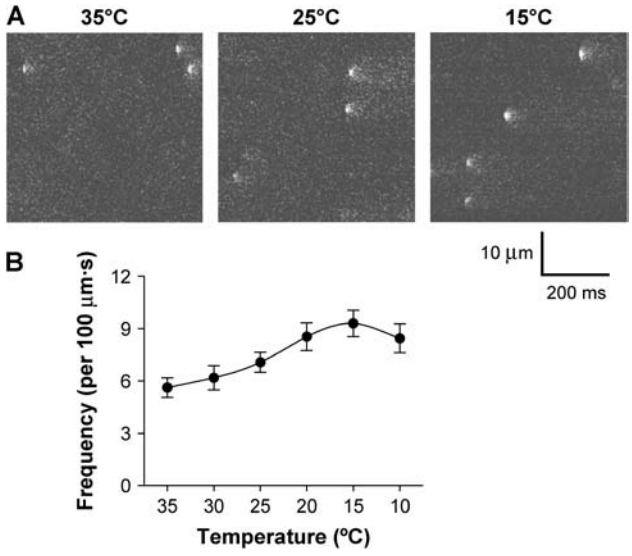

FIGURE 1 Confocal imaging of spontaneous Ca^{2+} sparks. (*A*). Representative line-scan images recorded in a rat ventricular myocyte at 35°C, 25°C, and 15°C (from *left* to *right*), respectively. For each image, time runs horizontally, and space runs vertically. (*B*). Temperature dependence of Ca^{2+} spark frequency ($n = 17$ cells each; $p < 0.05$). The frequency was calculated by dividing the total number of Ca^{2+} sparks by the product of distance (μm) and time (s) of line scanning.

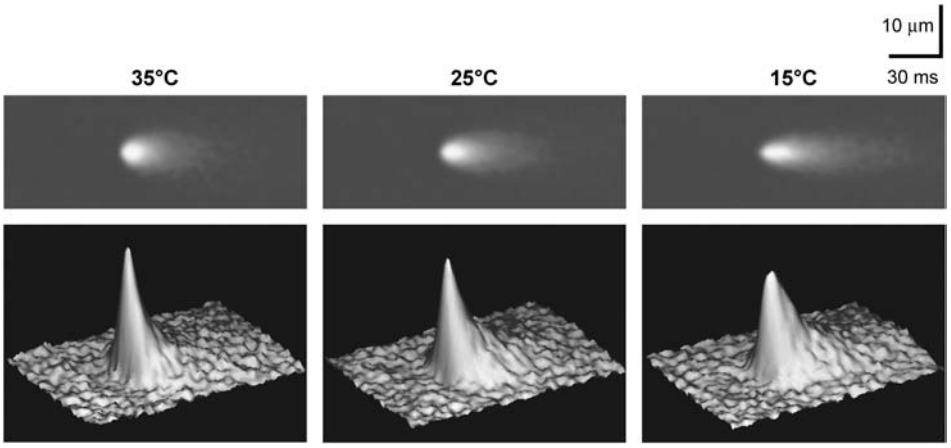

FIGURE 2 Two-dimensional and three-dimensional demonstration of the averages of 64 original Ca^{2+} sparks recorded at 35°C, 25°C, and 15°C, respectively. The original events were aligned by their takeoff times and spatial mass centers.

which would improve the signal/noise ratio by eightfold. The two-dimensional and three-dimensional images of the averaged data (Fig. 2) show that temperature modified both amplitude and spatiotemporal features of Ca^{2+} sparks.

The amplitude of Ca^{2+} sparks

Fig. 3 *A* illustrates the local Ca^{2+} profiles at 35°C, 25°C, and 15°C when the averaged sparks reached their peaks, which demonstrated that the lower the temperature, the lower the spark amplitude. Original data show that the amplitude of Ca^{2+} sparks, when expressed in $\Delta F/F_0$, was decreased significantly from 0.58 ± 0.02 at 35°C to 0.47 ± 0.01 at 10°C (Fig. 3 *B*, $p < 0.05$).

During the decline in temperature, the baseline (visualized as F_0) of intracellular free Ca^{2+} concentration ($[Ca^{2+}]_i$) would not remain constant (14,21). Therefore, the change of $\Delta F/F_0$ of Ca^{2+} sparks may not be comparable among different temperatures. To assess the underlying $\Delta[Ca^{2+}]_i$ of Ca^{2+} sparks, we determined the resting $[Ca^{2+}]_i$ by ratiometric confocal microscopy using indo-1 as the Ca^{2+} indicator. The measurement showed that resting $[Ca^{2+}]_i$ increased monotonically with lowering temperature (Fig. 3 *C*). Based on this measurement, we calculated the $\Delta[Ca^{2+}]_i$ of spark amplitude. As shown in Fig. 3 *D*, the $\Delta[Ca^{2+}]_i$ of Ca^{2+} sparks remained constant above 20°C and gradually lifted up at lower temperature range.

Spatiotemporal properties of Ca^{2+} sparks

It can be seen in the time courses of Ca^{2+} sparks (Fig. 4 *A*) that both the rise and decay became slower when the temperature was lowered. The FDHM, a commonly employed index of Ca^{2+} spark kinetics, increased monotonically from 17.0 ± 0.4 ms at 35°C to 24.3 ± 0.5 ms at 10°C (Fig. 4 *B*). By contrast, the FWHM of Ca^{2+} sparks, which reflexes

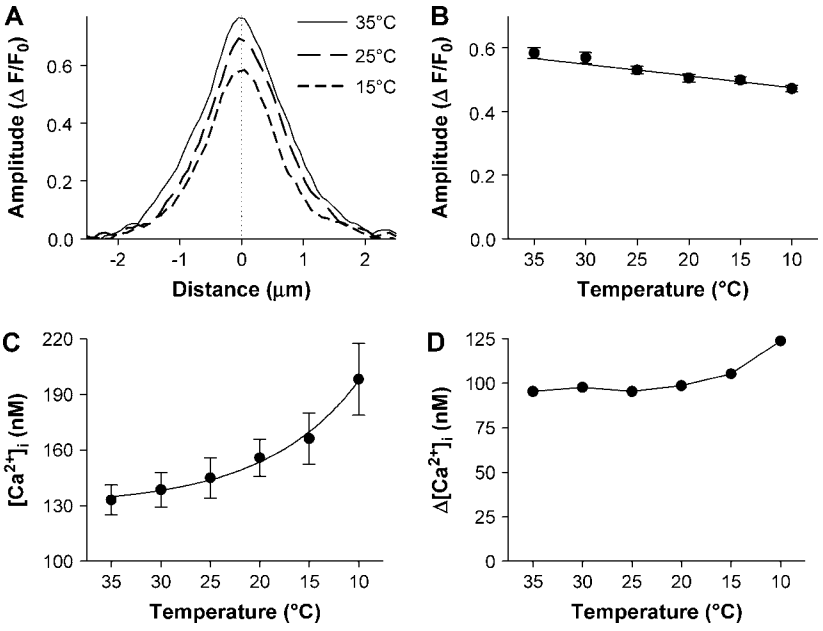

FIGURE 3 Temperature dependence of spark amplitude. (*A*). An overlay of the spatial profiles at the peak of the averaged sparks shown in Fig. 2. (*B*). Temperature dependence of spark amplitude (F/F_0). Each data point represents an average of more than 240 sparks from 17 cells in six animals ($p < 0.05$). (*C*). Temperature dependence of resting $[Ca^{2+}]_i$ in rat ventricular myocytes (n = nine cells from three animals; $p < 0.01$). (*D*). Ca^{2+} spark amplitude in terms of $\Delta[Ca^{2+}]_i$ was calculated from the data in *B* and *C* using Eq. 1.

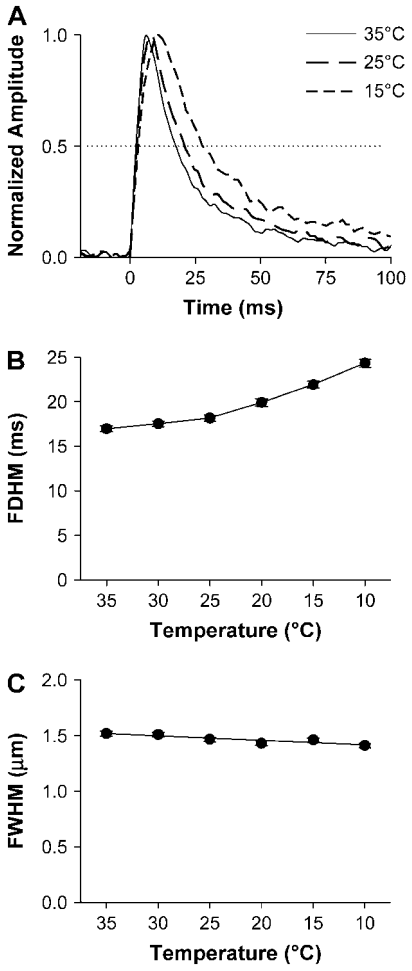

FIGURE 4 Temperature dependence of the temporal and spatial properties Ca^{2+} sparks. (*A*). An overlay of the time courses of the averaged sparks shown in Fig. 2. (*B*). Temperature dependence of FDHM of spark amplitude (F/F_0) ($p < 0.01$). (*C*). Temperature dependence of FWHM of Ca^{2+} sparks ($p > 0.05$).

spatial dispersion of Ca^{2+} sparks, changed little with temperature (Fig. 4 *C*).

Time-to-peak of Ca^{2+} sparks

During a Ca^{2+} spark, Ca^{2+} is released from a small number of RyRs and accumulates over time. The data showed that the time-to-peak of Ca^{2+} sparks exhibited bell-shaped distributions, which shifted rightward when temperature went down (Fig. 5 *A*). The average of time-to-peak increased from 9.7 ± 0.3 ms at 35°C to 13.4 ± 0.3 ms at 10°C (Fig. 5 *B*).

We noticed in Fig. 5 *B* that there was a break in slope at ~25°C. The ratio for every 10°C change (Q_{10}) was 1.05 between 25°C and 35°C but was increased to 1.19 between 10°C and 25°C. A similar phenomenon has previously been described for kinetic parameters of many membrane proteins, such as the turnover rate of sodium pumps (22) and the gating properties of ion channels (23). The discontinuous temperature dependence in Arrhenius plots has been attributed to a phase transition of membrane lipids, which alters the apparent activation energy (E_a) associated with the conformational change of membrane proteins. We speculated that a similar analysis might provide information about the energetic aspects of Ca^{2+} release channels. We plotted the natural logarithm of the kinetic index (k) of the RyR opening (represented by the reciprocal of time-to-peak) against the corresponding reciprocal of absolute temperature ($1/T$) (Fig. 5 *C*). The resulting Arrhenius plot could be best fit by two intersecting lines, each described by the Arrhenius equation

$$\ln k = \ln A - \frac{E_a}{RT}, \tag{3}$$

in which R is the gas constant and A is a fitting parameter. The intersection of fitted lines suggested that a transition of SR membrane might occur at 24.8°C. The fitting determined that the apparent E_a for RyR Ca^{2+} release is 5.2 or 14.6 kJ/mol, respectively, at temperatures higher or lower than the transition temperature.

Diffusion of local Ca^{2+}

After being released from RyRs, Ca^{2+} diffuses from its origin to adjacent intracellular space. To assess the effect of temperature on Ca^{2+} diffusion, we tracked the apparent wavefronts of Ca^{2+} spark by constructing mono-side contours that cut through the bottom 10% of the averaged Ca^{2+} sparks (Fig. 6 *A*, *symbols*). Before Ca^{2+} sparks reached their peak, the distance (x) of the apparent wavefront away from the Ca^{2+} origin was a function of time (t) that could be well described (Fig. 6 *A*, *lines*) by the Einstein Diffusion Equation:

$$x^2 = 2D_a t, \tag{4}$$

in which D_a is the apparent diffusion coefficient. By fitting the contour data to Eq. 4, we observed that D_a decreased monotonically with temperature (Fig. 6 *B*). By replacing the kinetic parameter k with dx/dt, the Arrhenius equation (Eq. 3) can be transformed to

$$\ln D_a = \ln(2tA^2) - \frac{2E_a}{RT}. \tag{5}$$

Linear fitting of $\ln D_a$ determined an E_a of 8.4 KJ/mol, corresponding to Q_{10} of 1.12 (Fig. 6 *C*).

Recovery of Ca^{2+} sparks

After the closure of RyRs, the local $[Ca^{2+}]_i$ declines with time due to diffusion and, possibly, active transports by SR Ca^{2+}-ATPase and Na^+-Ca^{2+} exchange. As Ca^{2+} diffusion and active transports have distinct thermodynamic properties, analysis of the temperature dependence may provide clues regarding how they contribute to the recovery from intracellular Ca^{2+} events. For this purpose, we measured the half-decay time, a commonly employed index of recovery

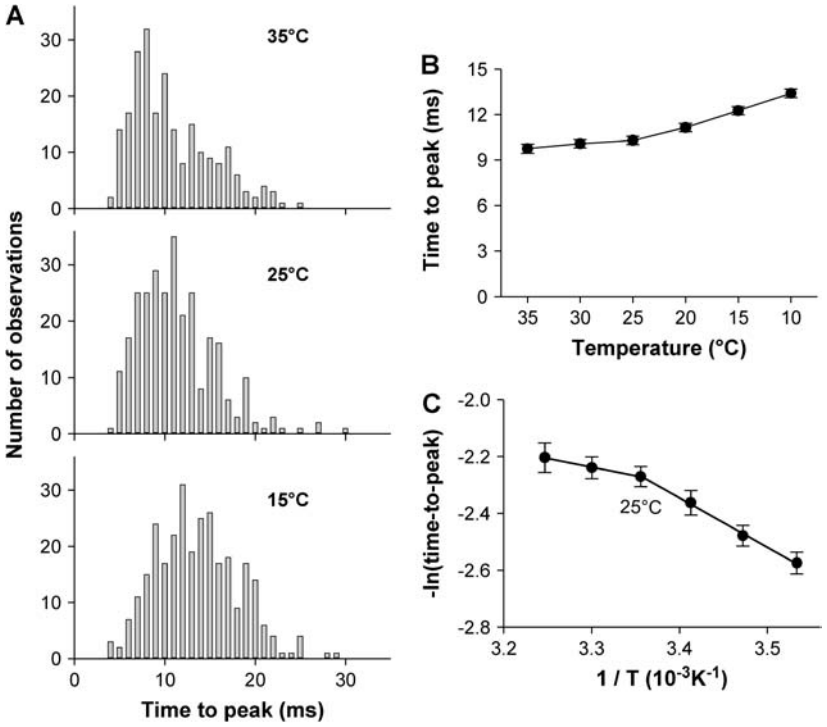

FIGURE 5 Thermodynamic analysis of RyR Ca^{2+} release duration. (*A*). Histograms showing the distributions of time-to-peak of Ca^{2+} sparks at 35°C, 25°C, and 15°C, respectively. (*B*). Temperature dependence of the time-to-peak of Ca^{2+} sparks ($p < 0.01$). Note the break of trend at ~25°C. (*C*). Arrhenius plot of the reciprocal of time-to-peak. The data were fitted by a combination of two lines with Eq. 3. Best fit was achieved by lines intersecting at 24.8°C.

kinetics. As shown in Fig. 7 *A*, the half-decay time increased monotonically with the decrease in temperature, indicating a slowing down in Ca^{2+} recovery. To quantify its thermodynamic property, we plotted the natural logarithm of its reciprocal against the reciprocal of absolute temperature. Fitting this Arrhenius plot (Fig. 7 *B*) yielded an apparent E_a of 9.2 kJ/mol, corresponding to Q_{10} of 1.14. This temperature sensitivity is similar to that of Ca^{2+} diffusion, but differs essentially with those of active transports. Therefore, Ca^{2+} diffusion is the major determinant in the early recovery process of Ca^{2+} sparks.

How about the late recovery phase? We then determined a late time constant by fitting the second half of decay in Ca^{2+} sparks. As shown in Fig. 7 *C*, the late time constant of Ca^{2+} sparks was prolonged by ~1-fold from 35°C to 10°C at a Q_{10} of 1.33. The Arrhenius plot of the corresponding rate constant (reciprocal of the time constant) determined that the apparent E_a for late recovery of Ca^{2+} sparks was 20.6 kJ/mol (Fig. 7 *D*), well above that of Ca^{2+} diffusion. Therefore, the role of active transports (24) is more important in determining the kinetics of the late, slow phase of Ca^{2+} spark recovery.

DISCUSSION

In this study, by characterizing Ca^{2+} spark properties over a range of temperatures, we have analyzed the factors that shaped up the temperature dependence of Ca^{2+} sparks and revealed relevant thermodynamic parameters involved in intracellular Ca^{2+} signals. The data provide a quantitative basis for interpreting intracellular Ca^{2+} signaling under various thermal conditions, including normal mammalian body temperature and hypothermia.

Gating properties of RyRs reflected in Ca^{2+} sparks

RyR is the Ca^{2+} release channel that mediates Ca^{2+} sparks in heart cells. Because its intracellular location prevents direct electrophysiological measurement, most of our knowledge about its channel properties has been based on in vitro measurements in artificial lipid bilayers (for review, see Fill and Copello (25)). In situ operation of RyRs could not be measured until the finding of Ca^{2+} spark, whose time-to-peak was suggested as an index of RyR open duration. Although an early mathematical deconvolution study of Ca^{2+} flux underlying a Ca^{2+} spark (26) raised a possibility that RyR Ca^{2+} release may outlast the rise phase of Ca^{2+} sparks, it was also pointed out that Ca^{2+} flux reconstruction from individual spark records is problematic due to a low signal/noise ratio (27). With improved quality of imaging enabled by the new generation of confocal microscopic technology, it was recently shown that the rise phase of in-focus Ca^{2+} sparks has the exponential kinetics expected from a square-waveform Ca^{2+} flux (28). Measurement of spark Ca^{2+} flux with a fast, low-affinity Ca^{2+} indicator combined with a slow Ca^{2+} buffer showed that Ca^{2+} release duration and spark time-to-peak are of the same value (29). Therefore, time-to-peak of Ca^{2+} sparks is by far the best approximation of RyR open duration in situ.

Temperature has been used as a tool to understand the kinetics and thermodynamics of ion channels (23,30,31). It

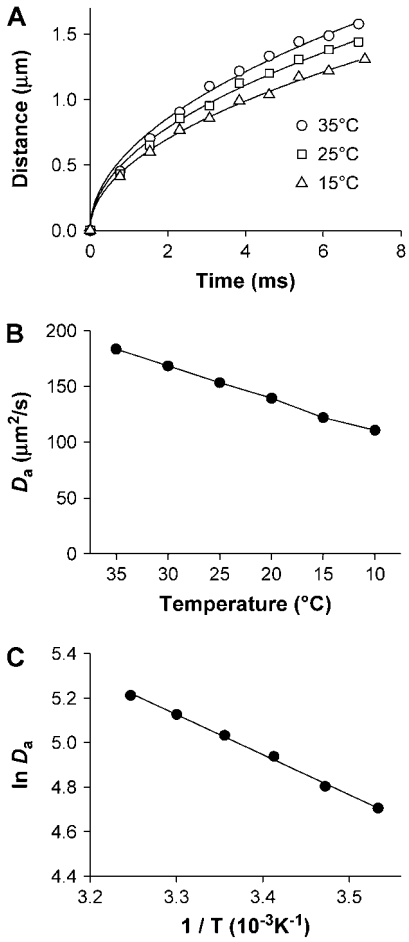

FIGURE 6 Temperature dependence of the spatial dispersion of spark wavefronts at bottom 10%. (*A*). Spatiotemporal wave front profiles of the Ca^{2+} sparks, each from the average of 64 original events. The curves represent the fitting to the data with Eq. 4. (*B*). Temperature dependence of the apparent diffusion coefficient D_a determined as in *A* ($p < 0.01$). (*C*). Thermodynamic analysis of D_a. The solid lines represent linear fitting with Eq. 5.

has been found that, for most ion channels, the temperature dependence of conductance does not differ significantly from that of a diffusion-limited process; the Q_{10} usually ranges between 1.1 ~ 1.5, whereas the gating, in general, shows much greater sensitivity to temperature with Q_{10} values ranging between 1.5 and 6 (32). For RyRs from sheep cardiac muscle incorporated in lipid bilayers, a decrease in temperature from 23°C to 5–10°C increases single RyR open probability (P_o) from 0.13 to 0.69 in the presence of 10 μM activating Ca^{2+} (33). As the increase in P_o results exclusively from an increase in channel open duration rather than the frequency of channel opening (33), the apparent Q_{10} for open duration of RyRs in vitro should be ~3. This value contrasts with the Q_{10} of 1.25 for RyRs gating in situ in a similar temperature range revealed by time-to-peak measurement in this study.

The difference in the temperature dependence of RyR in situ and in vitro parallels their distinct patterns in gating kinetics. It is known that a single RyR incorporated in lipid bilayers, as almost all other known ion channels, exhibits an exponential open duration distribution (34). This type of open duration distribution is determined by the thermodynamic reversibility of stochastic transition of channel status and is generally shared by all Markovian channels or channel groups that are usually uncoupled from external free energy (35,36). Even coupled gating of multiple RyRs in vitro still satisfies the thermodynamic reversibility, although the synchronized open duration is much prolonged compared to that of a single RyR (37). However, the time-to-peak of Ca^{2+} sparks usually exhibits a bell-shaped distribution, which cannot be explained based on any thermodynamic reversible scenario. We have therefore postulated a model in which the Ca^{2+}-induced Ca^{2+} release among adjacent RyRs in situ may couple a certain source of external energy, resulting in a thermodynamically irreversible mode of gating (28,29). In this study, we show that the apparent E_a (14.6 kJ/mol) for RyR Ca^{2+} release is indeed much lower than that estimated for RyRs gating in vitro (~70 kJ/mol, calculated based on Sitsapesan et al. (33)). We speculate that, among other possibilities, the difference of apparent E_a may possibly reflect the external free energy that drives the irreversible gating.

Temperature dependence involves multiple processes

At any temperature, the Ca^{2+} spark parameters, including amplitude, kinetics, and spatial dispersion, depend on the rates of many different processes, including RyR Ca^{2+} release, Ca^{2+} diffusion and buffering within intracellular microdomains, and Ca^{2+} transports by pumps and exchangers. Some of these rates, such as those of Na^+-Ca^{2+} exchangers (38,39) and SR Ca^{2+}-pumps (40) depend strongly on temperature, with apparent Q_{10} values ranging between 2 ~ 4, whereas others (e.g., Ca^{2+} diffusion) are likely to be far less sensitive to temperature with Q_{10} values <1.3. In the recovery phase of Ca^{2+} sparks, for example, both Ca^{2+} diffusion and active transports contribute to the decay of local $[Ca^{2+}]_i$ (24). However, the Q_{10} of the first half of recovery is similar to that of ion diffusion, whereas that of the second half becomes larger. This phenomenon indicates that Ca^{2+} spark recovery is initially dominated by fast equilibration of local Ca^{2+}. The role of active transports becomes more important in the slower phase of recovery.

When two or more rates contribute significantly in a process, their effects could be synergistic or offsetting. For example, due to slowed Ca^{2+} diffusion, the spatial dispersion became narrowed when temperature was lowered. However, this effect was largely compensated by prolonged Ca^{2+} release. As the result, the FWHM of Ca^{2+} sparks changed little with temperature. On the other hand, both

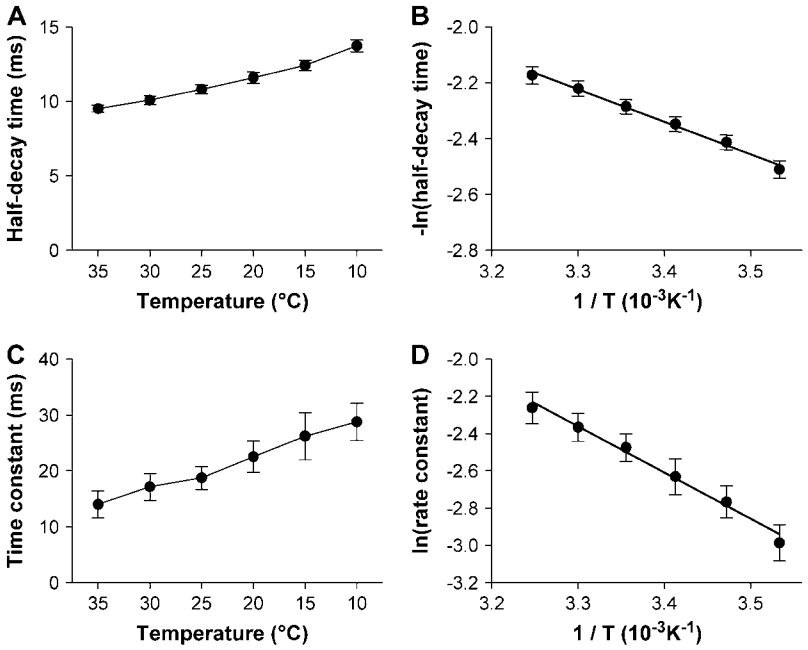

FIGURE 7 Thermodynamic analysis of recovery kinetics of Ca^{2+} sparks. (*A* and *C*). Temperature dependence of half-decay time (*A*) and late time constant (*C*) of Ca^{2+} sparks ($p < 0.01$). (*B* and *D*). Arrhenius plot of the reciprocal of half-decay time (*B*) and late time constant (*D*). The solid lines represent linear fitting with Eq. 3.

prolonged Ca^{2+} release and slowed Ca^{2+} diffusion tend to facilitate the local accumulation of Ca^{2+}. They are synergistic in determining the amplitude of Ca^{2+} sparks. However, the amplitude of Ca^{2+} sparks appears to be insensitive to temperature, implying that the Ca^{2+} release flux is attenuated when temperature is lowered. Although it is not presently known whether the number of RyRs participating in sparks is changed, in vitro studies have shown that the unitary current of RyRs in lipid bilayers indeed changes with temperature at a Q_{10} of 1.5 (33).

Temperature sensitivity of Ca^{2+} sparks and heart function

One of the common issues that have been discussed since the inception of Ca^{2+} sparks is the validity to interpret mammalian cardiac and muscular function using room temperature-measured Ca^{2+} sparks. This issue was recently visited by Ferrier et al. (10), who showed that Ca^{2+} sparks in mouse cardiomyocytes measured at 22°C are >1000% more in spark frequency, 42% higher in amplitude ($\Delta F/F_0$), and 43% longer in time-to-peak than those measured at 37°C, with half-decay time unchanged. Their results contrast with the 50% increase in frequency, 13% decrease (rather than increase) in $\Delta F/F_0$, 14% increase in time-to-peak, and 21% increase (rather than being unaltered) in half-decay time in our rat data during a comparable change in temperature. Several factors may be implicated in the high discrepancy between these two studies:

1. SR Ca^{2+} load. In resting cardiac myocytes from all tested species, including rats and mice, lowering temperature results in increased SR Ca^{2+} content (10,41,42). However, this does not mean that low temperature fortified the SR capability to uptake Ca^{2+}; rather, the increased SR load has to do with inhibited Na^+-pump activity at low temperature. The attenuated Na^+ handling (22) will shift the Ca^{2+} flux via Na^+-Ca^{2+} exchange. The resulted $[Ca^{2+}]_i$ elevation, which tends to load the SR even when Ca^{2+}-pump activity slows down at low temperature. Interestingly, the cooling-induced increase in spark frequency, which is sensitive to SR load, correlates well with the progressive elevation in resting $[Ca^{2+}]_i$ in rat cells but not in mouse cells (10).
2. Species-related difference. The relative strength of Na^+-Ca^{2+} exchange and SR Ca^{2+} pumping varies with species (1). Although the relative contributions of these two mechanisms in removing cytosol Ca^{2+} are similar in rat and mouse cardiomyocytes at 23°C (1), it is not known whether they differ at higher temperature. Besides, possible species difference in Ca^{2+}-sensing, gating, and luminal regulation of RyRs should also be taken into consideration.
3. Number of observations. In connection with the extreme infrequency of Ca^{2+} sparks at 37°C in mouse cardiomyocytes, only 19 sparks could be compared with those at 22°C (10). Given the highly variable nature of Ca^{2+} sparks, some of the observed temperature responses, such as the temperature insensitivity of half-decay time, may not be conclusive without further examination.

To ensure the accuracy of results, we measured >240 sparks for each data point in this study. We found that spark amplitude ($\Delta[Ca^{2+}]_i$) and FWHM are relatively insensitive to temperature. Although the resting $[Ca^{2+}]_i$, time-to-peak and half-decay times, and therefore FDHM, increase significantly

from 35°C to 10°C, they are only altered by 8%, 5%, 10%, and 7%, respectively, during the first 10°C change. Therefore, our data suggest that when cardiac Ca^{2+} sparks are measured at a room temperature around or above the transitional 25°C (so-called ''warm room''), they are basically acceptable to account for the heart function in mammals.

Below the critical temperature of 25°C, where the phase transition of membrane lipids occurs, membrane protein-mediated processes, including RyR gating, Ca^{2+} transport by Ca^{2+} pumps, and exchangers, encountered increased energetic barriers in conformational transitions and become more sensitive to temperature. A comparable change in temperature would cause more profound changes in Ca^{2+} spark kinetics and much more profound changes in kinetics of Ca^{2+} transients (14). As the result of prolonged and increased RyR Ca^{2+} release and truncated capability of intracellular Ca^{2+} handling, resting $[Ca^{2+}]_i$ becomes inhomeostatic (Fig. 3 *C*). In addition, low temperature also leads to a progressive loss in resting membrane potential (43), which will promote Ca^{2+} entry through the window current of L-type Ca^{2+} channels. These factors additively lead to Ca^{2+} overload in cytosol, resulting in incomplete relaxation and, eventually, loss of myocardial contractility. In hibernating mammals, however, the contractility can be maintained at a temperature near freezing point (13). It is thus intriguing how the cell system in hibernators is adapted to cope with these temperature-dependent issues.

CONCLUSIONS

In this study, we have characterized Ca^{2+} sparks systemically over a wide temperature range that covers both euthermic and hypothermic conditions. Whereas the amplitude and spatial dispersion of Ca^{2+} sparks are relatively insensitive to temperature, the spark kinetics slows down significantly due to prolonged RyR Ca^{2+} release duration and slowed Ca^{2+} diffusion under low temperature conditions. The temperature dependence of Ca^{2+} release duration reveals a lowered apparent E_a for RyRs gating in situ compared with that in vitro. The relative temperature insensitivity of Ca^{2+} spark parameters above ~25°C suggests that Ca^{2+} sparks measured at ''warm room'' temperatures are basically acceptable in elucidating mammalian heart functions.

The authors thank Ms. Shuhua Bai for technical assistance and Dr. Haihong Ye for constructive comments and suggestions on the manuscript.

This study was supported by National Natural Science Foundation of China (programs 30425035 and 30421004) and National Key Basic Research Program of Ministry of Science and Technology of China (973 Program 2004CB720007) to S.Q.W.

REFERENCES

1. Bers, D. M. 2001. Excitation-Contraction Coupling and Cardiac Contractile Force, 2nd ed. Kluwer Academic Publishers, Dordrecht, The Netherlands.
2. Berridge, M. J., M. D. Bootman, and H. L. Roderick. 2003. Calcium signalling: dynamics, homeostasis and remodelling. *Nat. Rev. Mol. Cell Biol.* 4:517–529.
3. Cheng, H., W. J. Lederer, and M. B. Cannell. 1993. Calcium sparks: elementary events underlying excitation-contraction coupling in heart muscle. *Science.* 262:740–744.
4. Lopez-Lopez, J. R., P. S. Shacklock, C. W. Balke, and W. G. Wier. 1994. Local, stochastic release of Ca2+ in voltage-clamped rat heart cells: visualization with confocal microscopy. *J. Physiol.* 480:21–29.
5. Tsugorka, A., E. Rios, and L. A. Blatter. 1995. Imaging elementary events of calcium release in skeletal muscle cells. *Science.* 269:1723–1726.
6. Nelson, M. T., H. Cheng, M. Rubart, L. F. Santana, A. D. Bonev, H. J. Knot, and W. J. Lederer. 1995. Relaxation of arterial smooth muscle by calcium sparks. *Science.* 270:633–637.
7. Koizumi, S., M. D. Bootman, L. K. Bobanovic, M. J. Schell, M. J. Berridge, and P. Lipp. 1999. Characterization of elementary Ca2+ release signals in NGF-differentiated PC12 cells and hippocampal neurons. *Neuron.* 22:125–137.
8. Haak, L. L., L. S. Song, T. F. Molinski, I. N. Pessah, H. Cheng, and J. T. Russell. 2001. Sparks and puffs in oligodendrocyte progenitors: cross talk between ryanodine receptors and inositol trisphosphate receptors. *J. Neurosci.* 21:3860–3870.
9. Wier, W. G., H. E. D. J. terKeurs, E. Marban, W. D. Gao, and C. W. Balke. 1997. Ca2+ 'sparks' and waves in intact ventricular muscle resolved by confocal imaging. *Circ. Res.* 81:462–469.
10. Ferrier, G. R., R. H. Smith, and S. E. Howlett. 2003. Calcium sparks in mouse ventricular myocytes at physiological temperature. *Am. J. Physiol. Heart Circ. Physiol.* 285:H1495–H1505.
11. Chao, I. 1959. The recovery of dogs from deep hypothermia. *Acta Sci. Nat. Univ. Pekinensis.* 5:99–102.
12. Liu, B., B. Wohlfart, and B. W. Johansson. 1990. Effects of low temperature on contraction in papillary muscles from rabbit, rat, and hedgehog. *Cryobiology.* 27:539–546.
13. Wang, S. Q., Y. H. Huang, K. S. Liu, and Z. Q. Zhou. 1997. Dependence of myocardial hypothermia tolerance on sources of activator calcium. *Cryobiology.* 35:193–200.
14. Wang, S. Q., Z. Q. Zhou, and H. Qian. 2000. Recording of calcium transient and analysis of calcium removal mechanisms in cardiac myocytes from rats and ground squirrels. *Sci. China C Life Sci.* 43: 191–199.
15. Wang, S. Q., and Z. Q. Zhou. 1999. Alpha-stat calibration of indo-1 fluorescence and measurement of intracellular free calcium in rat ventricular cells at different temperatures. *Life Sci.* 65:871–877.
16. Zhou, Y. Y., S. Q. Wang, W. Z. Zhu, A. Chruscinski, B. K. Kobilka, B. Ziman, S. Wang, E. G. Lakatta, H. Cheng, and R. P. Xiao. 2000. Culture and adenoviral infection of adult mouse cardiac myocytes: methods for cellular genetic physiology. *Am. J. Physiol. Heart Circ. Physiol.* 279:H429–H436.
17. Cheng, H., L. S. Song, N. Shirokova, A. Gonzalez, E. G. Lakatta, E. Rios, and M. D. Stern. 1999. Amplitude distribution of calcium sparks in confocal images: theory and studies with an automatic detection method. *Biophys. J.* 76:606–617.
18. Hollingworth, S., J. Peet, W. K. Chandler, and S. M. Baylor. 2001. Calcium sparks in intact skeletal muscle fibers of the frog. *J. Gen. Physiol.* 118:653–678.
19. Lattanzio, F. A. Jr. 1990. The effects of pH and temperature on fluorescent calcium indicators as determined with Chelex-100 and EDTA buffer systems. *Biochem. Biophys. Res. Commun.* 171:102–108.
20. Harkins, A. B., N. Kurebayashi, and S. M. Baylor. 1993. Resting myoplasmic free calcium in frog skeletal muscle fibers estimated with fluo-3. *Biophys. J.* 65:865–881.
21. Liu, B., L. C. Wang, and D. D. Belke. 1991. Effect of low temperature on the cytosolic free Ca2+ in rat ventricular myocytes. *Cell Calcium.* 12:11–18.

22. Kairane, C., K. Roots, T. Uusma, N. Bogdanovic, E. Karelson, S. Koks, and M. Zilmer. 2002. Regulation of the frontocortical sodium pump by Na+ in Alzheimer's disease: difference from the age-matched control but similarity to the rat model. *FEBS Lett.* 531:241–244.

23. Bennetts, B., M. L. Roberts, A. H. Bretag, and G. Y. Rychkov. 2001. Temperature dependence of human muscle ClC-1 chloride channel. *J. Physiol.* 535:83–93.

24. Gomez, A. M., H. Cheng, W. J. Lederer, and D. M. Bers. 1996. Ca2+ diffusion and sarcoplasmic reticulum transport both contribute to [Ca2+]i decline during Ca2+ sparks in rat ventricular myocytes. *J. Physiol.* 496:575–581.

25. Fill, M., and J. A. Copello. 2002. Ryanodine receptor calcium release channels. *Physiol. Rev.* 82:893–922.

26. Lukyanenko, V., T. F. Wiesner, and S. Gyorke. 1998. Termination of Ca2+ release during Ca2+ sparks in rat ventricular myocytes. *J. Physiol. (Lond.).* 507:667–677.

27. Soeller, C., and M. B. Cannell. 2002. Estimation of the sarcoplasmic reticulum Ca2+ release flux underlying Ca2+ sparks. *Biophys. J.* 82:2396–2414.

28. Wang, S. Q., M. D. Stern, E. Rios, and H. Cheng. 2004. The quantal nature of Ca2+ sparks and in situ operation of the ryanodine receptor array in cardiac cells. *Proc. Natl. Acad. Sci. USA.* 101:3979–3984.

29. Wang, S. Q., L. S. Song, L. Xu, G. Meissner, E. G. Lakatta, E. Rios, M. D. Stern, and H. Cheng. 2002. Thermodynamically irreversible gating of ryanodine receptors in situ revealed by stereotyped duration of release in Ca(2+) sparks. *Biophys. J.* 83:242–251.

30. Bamberg, E., and P. Lauger. 1974. Temperature-dependent properties of gramicidin A channels. *Biochim. Biophys. Acta.* 367:127–133.

31. Rodriguez, B. M., D. Sigg, and F. Bezanilla. 1998. Voltage gating of Shaker K+ channels. The effect of temperature on ionic and gating currents. *J. Gen. Physiol.* 112:223–242.

32. DeCoursey, T. E., and V. V. Cherny. 1998. Temperature dependence of voltage-gated H+ currents in human neutrophils, rat alveolar epithelial cells, and mammalian phagocytes. *J. Gen. Physiol.* 112:503–522.

33. Sitsapesan, R., R. A. Montgomery, K. T. MacLeod, and A. J. Williams. 1991. Sheep cardiac sarcoplasmic reticulum calcium-release channels: modification of conductance and gating by temperature. *J. Physiol.* 434:469–488.

34. Xu, L., and G. Meissner. 1998. Regulation of cardiac muscle Ca2+ release channel by sarcoplasmic reticulum lumenal Ca2+. *Biophys. J.* 75:2302–2312.

35. Colquhoun, D., and A. G. Hawkes. 1995. The principles of the stochastic interpretation of ion-channel mechanisms. *In* Single Channel Recording, 2nd ed. B. Sakmann and E. Neher, editors. Plenum Press, New York. 397–482.

36. Rengifo, J., R. Rosales, A. Gonzalez, H. Cheng, M. D. Stern, and E. Rios. 2002. Intracellular Ca(2+) release as irreversible Markov process. *Biophys. J.* 83:2511–2521.

37. Marx, S. O., J. Gaburjakova, M. Gaburjakova, C. Henrikson, K. Ondrias, and A. R. Marks. 2001. Coupled gating between cardiac calcium release channels (ryanodine receptors). *Circ. Res.* 88:1151–1158.

38. Kimura, J., S. Miyamae, and A. Noma. 1987. Identification of sodium-calcium exchange current in single ventricular cells of guinea-pig. *J. Physiol.* 384:199–222.

39. Powell, T., A. Noma, T. Shioya, and R. Z. Kozlowski. 1993. Turnover rate of the cardiac Na(+)-Ca2+ exchanger in guinea-pig ventricular myocytes. *J. Physiol.* 472:45–53.

40. Horiuti, K. 1988. Mechanism of contracture on cooling of caffeine-treated frog skeletal muscle fibres. *J. Physiol.* 398:131–148.

41. Shattock, M. J., and D. M. Bers. 1987. Inotropic response to hypothermia and the temperature-dependence of ryanodine action in isolated rabbit and rat ventricular muscle: implications for excitation-contraction coupling. *Circ. Res.* 61:761–771.

42. Puglisi, J. L., R. A. Bassani, J. W. Bassani, J. N. Amin, and D. M. Bers. 1996. Temperature and relative contributions of Ca transport systems in cardiac myocyte relaxation. *Am. J. Physiol.* 270:H1772–H1778.

43. Wang, S. Q., H. M. Cao, and Z. Q. Zhou. 1997. Temperature dependence of the myocardial excitability of ground squirrel and rat. *J. Therm. Biol.* 22:195–199.